

Vibrationally dependent electron-electron interactions in resonant electron transport through single-molecule junctions

A. Erpenbeck,¹ R. Härtle,² M. Bockstedte,¹ and M. Thoss¹¹*Institut für Theoretische Physik und Interdisziplinäres Zentrum für Molekulare Materialien, Friedrich-Alexander-Universität Erlangen-Nürnberg, Staudtstrasse 7/B2, D-91058 Erlangen, Germany*²*Institut für Theoretische Physik, Georg-August-Universität Göttingen, Friedrich-Hund-Platz 1, D-37077 Göttingen, Germany*

(Received 10 August 2015; revised manuscript received 18 December 2015; published 15 March 2016)

We investigate the role of electronic-vibrational coupling in resonant electron transport through single-molecule junctions, taking into account that the corresponding coupling strengths may depend on the charge and excitation state of the molecular bridge. Within an effective-model Hamiltonian approach for a molecule with multiple electronic states, this requires to extend the commonly used model and include vibrationally dependent electron-electron interaction. We use Born-Markov master equation methods and consider selected models to exemplify the effect of the additional interaction on the transport characteristics of a single-molecule junction. In particular, we show that it has a significant influence on local cooling and heating mechanisms, it may result in negative differential resistance, and it may cause pronounced asymmetries in the conductance map of a single-molecule junction.

DOI: [10.1103/PhysRevB.93.115421](https://doi.org/10.1103/PhysRevB.93.115421)

I. INTRODUCTION

Electron transport through a single-molecule junction constitutes a complex many-body problem. Electronic and vibrational degrees of freedom of a molecular conductor are often strongly correlated, in particular in nonequilibrium states at higher bias voltages [1–22]. The investigation of coupling between electronic and nuclear degrees of freedom in nanostructures under nonequilibrium conditions has been of great interest recently and revealed a wealth of physical phenomena such as rectification [2,23–26], vibrationally induced decoherence [26–29], negative differential resistance [26,30–34], and signatures of multistability [35–38].

Most theoretical studies of vibrationally coupled electron transport in molecular junctions have employed a simplified model of a molecule with linear coupling of the electronic degrees of freedom to vibrational modes described in the harmonic approximation [1,34,39–41]. More realistic extensions involve the study of anharmonic nuclear potentials [31,42–48]. The description of systems with multiple electronic states [17] often requires to include the Coulomb interaction between electrons. General first-principles approaches to electron-electron and electronic-vibrational interactions, as outlined in, e.g., Ref. [49], can be pursued, however at the expense of the simplicity provided by a model Hamiltonian. Within the realm of model Hamiltonians, an improvement toward more realistic models includes a dependence of the electron-electron interaction on the nuclear geometry to mimic the adiabatic Born-Oppenheimer surfaces of the molecule under investigation [50–53]. This results in vibrationally dependent electron-electron interactions. The study of this effect and its manifestation in transport characteristics of molecular junctions is the main subject of this article. The importance of vibrationally dependent electron-electron interactions has already been realized, for example, in the context of the Hubbard model approach to electron-electron interaction in molecules [50,53] in studies of dissociation in colloidal quantum dot systems [52] and current-induced dissociation of molecules [51].

The outline of this article is as follows: The theoretical methodology is introduced in Sec. II, including the model

Hamiltonian of the molecular junctions, the master equation approach used to describe charge transport, and a discussion of the relevance of vibrationally dependent electron-electron interactions. In Sec. III, we analyze the effects and manifestation of vibrationally dependent electron-electron interactions in transport characteristics. To that end, we consider selected model systems, including scenarios with symmetric and asymmetric molecule-lead coupling.

II. THEORETICAL METHODOLOGY

A. Model Hamiltonian

The starting point of our study is a generic model Hamiltonian, which is commonly used to describe the molecular bridge in a molecular junction [1,16,34,40,54,55],

$$H_M = H_{\text{nuc}} + H_{\text{el}}(\mathbf{R})$$

with

$$H_{\text{nuc}} = \sum_{\alpha} \Omega_{\alpha} a_{\alpha}^{\dagger} a_{\alpha}, \quad (1)$$

$$H_{\text{el}}(\mathbf{R}) = \sum_m \epsilon_m(\mathbf{R})(d_m^{\dagger} d_m - \delta_m) + \sum_{m < n} U_{mn}(\mathbf{R})(d_m^{\dagger} d_m - \delta_m)(d_n^{\dagger} d_n - \delta_n). \quad (2)$$

Here, H_{nuc} is the Hamiltonian describing the nuclear motion within the harmonic approximation. Thereby, Ω_{α} denotes the frequency of mode α , and a_{α}^{\dagger} and a_{α} are the corresponding creation and annihilation operators, respectively. $H_{\text{el}}(\mathbf{R})$ describes the electronic degrees of freedom of the molecule and depends parametrically on the nuclear coordinates \mathbf{R} . For simplicity, we do not consider the spin explicitly. $\epsilon_m(\mathbf{R})$ denotes the energy of the molecular orbital m , which depends on the nuclear coordinates, and d_m^{\dagger} and d_m are the corresponding fermionic creation and annihilation operators, respectively. The parameters δ_m distinguish between single-particle states that are occupied ($\delta_m = 1$) or unoccupied ($\delta_m = 0$) in the ground state of the neutral molecule, which serves as a reference state.

The last line in Eq. (2) describes the Coulomb interaction between two electrons on the molecule employing an effective model. A similar Coulomb interaction term, which depends on the nuclear coordinates, has already been proposed and investigated in Ref. [51]. Notice that $\epsilon_m(\mathbf{R})$ and $U_{mn}(\mathbf{R})$ are model functions, which are chosen such that they reproduce the potential-energy surfaces of the corresponding electronic states of the molecule (*vide infra*).

Derivations of the representation of the molecular Hamiltonian in second quantization similar to Eq. (2) can be found, for example, in Refs. [39,40,56–60]. In particular, Refs. [39,56] offer a rigorous derivation including nonadiabatic coupling between different states in the molecule. In the present paper, we focus on the effects of vibrationally dependent electron-electron interaction. Toward that end, we study model systems for physically relevant situations, where the neglect of nonadiabatic coupling is justified, i.e., the adiabatic approximation is valid. Nonadiabatic effects have been investigated in detail in previous work, e.g., in Refs. [26,41,61–64]. The study of the combined effect of vibrationally dependent electron-electron interaction and nonadiabatic coupling is an interesting topic for future research.

In accordance with the harmonic approximation employed for the nuclear degrees of freedom of the molecule, we expand the orbital energies, which enter the electronic part of the Hamiltonian, about the equilibrium geometry \mathbf{R}_0 of the reference state

$$\begin{aligned} \epsilon_m(\mathbf{R}) &= \epsilon_m(\mathbf{R}_0) + \sum_{\alpha} \left. \frac{\partial \epsilon_m(\mathbf{R})}{\partial Q_{\alpha}} \right|_{\mathbf{R}=\mathbf{R}_0} Q_{\alpha} + \dots \\ &\approx \epsilon_m + \sum_{\alpha} \lambda_{m\alpha} Q_{\alpha}. \end{aligned} \quad (3)$$

Thereby, $Q_{\alpha} = \frac{1}{\sqrt{2}}(a_{\alpha} + a_{\alpha}^{\dagger})$ is the dimensionless displacement of vibrational mode α , and $\lambda_{m\alpha}$ denote the electronic-vibrational coupling constants. Similarly, we expand the Coulomb interaction about \mathbf{R}_0 and arrive at an approximate expression for the electron-electron interaction,

$$\begin{aligned} U_{mn}(\mathbf{R}) &= U_{mn}(\mathbf{R}_0) + \sum_{\alpha} \left. \frac{\partial U_{mn}(\mathbf{R})}{\partial Q_{\alpha}} \right|_{\mathbf{R}=\mathbf{R}_0} Q_{\alpha} + \dots \\ &\approx U_{mn} + \sum_{\alpha} W_{m\alpha} Q_{\alpha}. \end{aligned} \quad (4)$$

Here, $W_{m\alpha}$ denotes the vibrationally dependent part of the electron-electron interaction. As a result, the total Hamiltonian of the molecular bridge used in the transport calculations is given by

$$\begin{aligned} H_S &= \sum_{\alpha} \Omega_{\alpha} a_{\alpha}^{\dagger} a_{\alpha} + \sum_m \epsilon_m (d_m^{\dagger} d_m - \delta_m) \\ &+ \sum_{m < n} U_{mn} (d_m^{\dagger} d_m - \delta_m) (d_n^{\dagger} d_n - \delta_n) \\ &+ \sum_{m\alpha} \lambda_{m\alpha} Q_{\alpha} (d_m^{\dagger} d_m - \delta_m) \\ &+ \sum_{m < n, \alpha} W_{m\alpha} Q_{\alpha} (d_m^{\dagger} d_m - \delta_m) (d_n^{\dagger} d_n - \delta_n). \end{aligned} \quad (5)$$

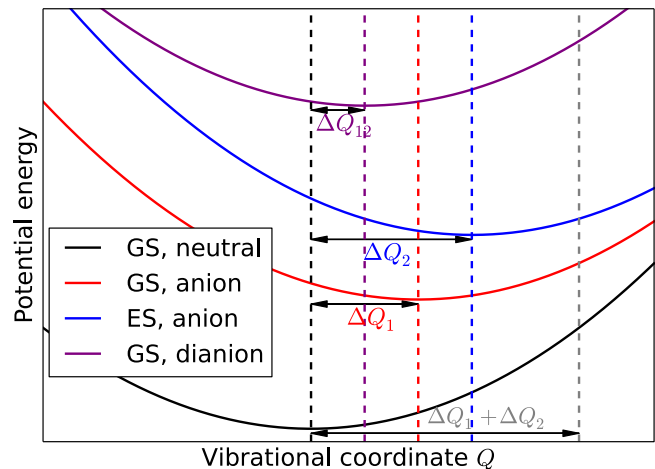


FIG. 1. Scheme of potential energy surfaces of the molecular bridge corresponding to the ground state (GS) and first excited state (ES) of the neutral molecule, its anion, and the dianion. The equilibrium geometry of the respective molecular states is marked by dashed vertical lines of the same color, and the displacement of the equilibrium geometry with respect to the ground state of the neutral molecule is shown by black arrows.

It includes electron-electron interactions U_{mn} , electronic-vibrational coupling $\lambda_{m\alpha}$, and vibrationally dependent electron-electron interactions $W_{m\alpha}$.

While the influence of electron-electron interactions and electronic-vibrational coupling on transport in molecular junctions has been studied in detail before [1,65], vibrationally dependent electron-electron interactions have so far only been considered in different contexts [50–52]. We first discuss their physical origin. The potential energy surfaces (PESs) of a generic one-dimensional model for a molecular junction are depicted in Fig. 1, where the solid black line is associated with the ground state of the neutral molecule, the solid red line with the ground state of the respective anion, the solid blue line with the first excited state of the anion, and the solid purple line with the ground state of the dianion. The minima of these PESs represent the equilibrium geometry of the nuclei, highlighted by dashed vertical lines. The equilibrium geometry of the nuclei changes upon charging or excitation of the molecule. This shift of the equilibrium geometry is a signature of electronic-vibrational coupling. For example, the shift of the equilibrium geometry of the ground state of the anion with respect to the ground state of the neutral molecule is given by $\Delta Q_1 = 2\lambda_{11}/\Omega_1$. Similarly, the equilibrium geometry of the first excited state of the anion is shifted by $\Delta Q_2 = 2\lambda_{21}/\Omega_1$ with respect to the ground state of the neutral molecule. Without vibrationally dependent electron-electron interactions, the equilibrium geometry of the nuclei in the ground state of the dianion would be shifted by $\Delta Q_{12} = \Delta Q_1 + \Delta Q_2 = 2(\lambda_{11} + \lambda_{21})/\Omega_1$ with respect to the ground state of the neutral molecule, i.e., it would be fixed by the parameters of the PES of the singly charged molecule. However, the equilibrium geometry of the nuclei of the dianion is not necessarily correctly described by this shift. The actual nuclear displacement can be characterized by an additional parameter via $\Delta Q_{12} = \Delta Q_1 + \Delta Q_2 + 2W_{121}/\Omega_1$.

This shows that vibrationally dependent electron-electron interaction accounts for additional shifts of the equilibrium geometry of the nuclei that occur if a state differs by the occupation of more than one single-particle state from the reference state.

In general, there is a direct relation between the PESs of the different electronic states, which can be calculated from first principles using various electronic-structure methods, and the model parameter ϵ_m , $\lambda_{m\alpha}$, U_{mn} , and $W_{mn\alpha}$. This will be demonstrated using the above-mentioned effective model, consisting of two electronic states and considering, for simplicity, a single vibrational mode Q (Fig. 1). Within our model, the PESs for the different electronic states are given by $\mathcal{V}_{\text{GS neutral}}(Q) = \frac{\Omega}{2}Q^2$ (electronic ground state of the neutral molecule), $\mathcal{V}_{\text{GS anion}}(Q) = \frac{\Omega}{2}Q^2 + \epsilon_1 + \lambda_1 Q$ (ground state of the anion), $\mathcal{V}_{\text{ES anion}}(Q) = \frac{\Omega}{2}Q^2 + \epsilon_2 + \lambda_2 Q$ (excited state of the anion), and $\mathcal{V}_{\text{GS dianion}}(Q) = \frac{\Omega}{2}Q^2 + \epsilon_1 + \lambda_1 Q + \epsilon_2 + \lambda_2 Q + U_{12} + W_{12}Q$ (ground state of the dianion). Assuming PESs obtained from *ab initio* calculations, the model parameters can be obtained from the following relations for the derivatives of the PESs at the equilibrium geometry of the neutral molecule:

$$\lambda_1 = \left. \frac{\partial \mathcal{V}_{\text{GS anion}}(Q)}{\partial Q} \right|_{Q=0}, \quad (6)$$

$$\lambda_2 = \left. \frac{\partial \mathcal{V}_{\text{ES anion}}(Q)}{\partial Q} \right|_{Q=0}, \quad (7)$$

$$W_{12} = \left. \frac{\partial \mathcal{V}_{\text{GS dianion}}(Q)}{\partial Q} \right|_{Q=0} - \lambda_1 - \lambda_2. \quad (8)$$

The generalization of this consideration to other electronic states and multiple vibrational modes is straightforward.

The interaction parameters $\lambda_{m\alpha}$, U_{mn} , and $W_{mn\alpha}$ depend on the specific molecule under consideration and can vary significantly [40,50,51,57,59,66,67]. Below, we consider representative models. Varying the parameter $W_{mn\alpha}$, we analyze the role of vibrationally dependent electron-electron interaction, which is the focus of the present paper. Based on the discussion above, we expect a pronounced influence of vibrationally dependent electron-electron interaction on the transport properties for molecules, where the charging/decharging process alters the bonding structure of the molecule. This is the case, for example, in molecules where transport involves the population of antibonding states or the depopulation of bonding states. Furthermore, organometallic compounds, such as transition-metal complexes, are known to show dramatic structural changes upon charging [68].

The molecule in a molecular junction is coupled to two electrodes, which we model by noninteracting electrons,

$$H_{L/R} = \sum_{k \in L/R} \epsilon_k c_k^\dagger c_k, \quad (9)$$

that are located on the left (L) and the right (R) electrode, respectively. The molecule-lead coupling can be described by

$$H_{\text{SL/SR}} = \sum_{m \in M, k \in L/R} V_{mk} c_k^\dagger d_m + \text{H.c.}, \quad (10)$$

which allows for electron exchange processes between the molecule and the leads and determines the level-width function,

$$\Gamma_{L/Rmn}(\epsilon) = 2\pi \sum_{k \in L/R} V_{mk} V_{nk}^* \delta(\epsilon - \epsilon_k). \quad (11)$$

Throughout this article, the leads are modeled as semi-infinite tight-binding chains with intersite coupling strength β . The corresponding level-width function is given by

$$\Gamma_{L/Rmn}(\epsilon) = \frac{\nu_{L/Rm} \nu_{L/Rn}^*}{\beta^2} \Theta(4\beta^2 - x^2) \sqrt{4\beta^2 - x^2}, \quad (12)$$

with $x = \epsilon - \mu_{L/R}$ and the Heaviside step function Θ [65,69,70]. Similar to V_{mk} , the parameters $\nu_{L/Rm}$ describe the coupling between the molecular orbital m and the respective lead. For simplicity, we neglect a dependency of the molecule-lead coupling on the nuclear degrees of freedom or the charge state of the molecule, and we assume, furthermore, a symmetric drop of bias voltage $\mu_L = -\mu_R = \Phi/2$.

The overall Hamiltonian used to describe a single-molecule contact is given by

$$H = H_S + H_L + H_R + H_{\text{SL}} + H_{\text{SR}}. \quad (13)$$

B. Effective population-dependent electronic-vibrational coupling

To understand the basic mechanism of vibrationally dependent electron-electron interactions, it is expedient to diagonalize the molecular part of the Hamiltonian H_S . Toward that end, we employ a generalized small polaron transformation [55,67,71,72] of the Hamiltonian

$$\bar{H} = e^S H e^{-S} \quad (14)$$

with

$$S = -i \sum_{m\alpha} \frac{\lambda_{m\alpha}}{\Omega_\alpha} (d_m^\dagger d_m - \delta_m) P_\alpha - i \sum_{m < n\alpha} \frac{W_{mn\alpha}}{\Omega_\alpha} (d_m^\dagger d_m - \delta_m)(d_n^\dagger d_n - \delta_n) P_\alpha \quad (15)$$

and we obtain

$$\bar{H} = \bar{H}_S + \bar{H}_B + \bar{H}_{\text{SB}}, \quad (16a)$$

$$\begin{aligned} \bar{H}_S &= \sum_m \bar{\epsilon}_m (d_m^\dagger d_m - \delta_m) + \sum_\alpha \Omega_\alpha a_\alpha^\dagger a_\alpha \\ &+ \sum_{m < n} \bar{U}_{mn} (d_m^\dagger d_m - \delta_m)(d_n^\dagger d_n - \delta_n), \end{aligned} \quad (16b)$$

$$\bar{H}_{\text{SB}} = \sum_{m \in M, k \in L/R} (V_{mk} c_k^\dagger d_m X_m + \text{H.c.}), \quad (16c)$$

$$\bar{H}_B = \bar{H}_L + \bar{H}_R = \sum_{k \in L/R} \epsilon_k c_k^\dagger c_k. \quad (16d)$$

The transformed Hamiltonian \bar{H} has no explicit electronic-vibrational or vibrationally dependent electron-electron interaction terms. The effect of these interactions is subsumed in the polaron-shifted energy levels,

$$\bar{\epsilon}_m = \epsilon_m - \sum_\alpha (\lambda_{m\alpha}^2 / \Omega_\alpha), \quad (17)$$

altered electron-electron interactions,

$$\bar{U}_{mn} = U_{mn} - 2 \sum_{\alpha} (\lambda_{m\alpha} \lambda_{n\alpha} / \Omega_{\alpha}) - 2 \sum_{\alpha} \frac{W_{m\alpha} (\lambda_{m\alpha} + \lambda_{n\alpha})}{\Omega_{\alpha}} - \sum_{\alpha} \frac{W_{m\alpha}^2}{\Omega_{\alpha}}, \quad (18)$$

and renormalized molecule-lead coupling matrix elements V_{mk} that are dressed by the shift operators,

$$X_m = \exp \left[i \sum_{\alpha} \left(\frac{\lambda_{m\alpha}}{\Omega_{\alpha}} + \sum_{n \neq m} \frac{W_{m\alpha}}{\Omega_{\alpha}} (d_n^{\dagger} d_n - \delta_n) \right) P_{\alpha} \right]. \quad (19)$$

Similar to the way the bare electronic-vibrational interaction $\lambda_{m\alpha}$ influences the electron-electron interaction [$U_{mn} \rightarrow \bar{U}_{mn} - 2 \sum_{\alpha} (\lambda_{m\alpha} \lambda_{n\alpha} / \Omega_{\alpha})$], the vibrationally dependent electron-electron interaction leads to coupling terms proportional to $d_m^{\dagger} d_m d_n^{\dagger} d_n d_p^{\dagger} d_p$ ($m \neq n \neq p$) and $d_m^{\dagger} d_m d_n^{\dagger} d_n d_p^{\dagger} d_p d_q^{\dagger} d_q$ ($m \neq n \neq p \neq q$) in \bar{H} . In the two-level models considered below, such terms do not contribute.

Aside from an additional renormalization of the bare electron-electron interaction strengths, $U_{mn} \rightarrow \bar{U}_{mn}$, which induces no qualitatively new effects compared to the case with $W_{m\alpha} = 0$, vibrationally dependent electron-electron interactions affect, in particular, the structure of the shift operators X_m . Instead of c -numbered electronic-vibrational coupling strengths, $\lambda_{m\alpha}$, the shift operators X_m involve effective electronic-vibrational coupling strengths

$$\tilde{\lambda}_{m\alpha} = \lambda_{m\alpha} + \sum_{n \neq m} W_{m\alpha} (d_n^{\dagger} d_n - \delta_n) \quad (20)$$

that include the electronic occupation operators ($d_n^{\dagger} d_n - \delta_n$) with respect to all single-particle states but the m th one. As a result, the effective electronic-vibrational coupling strengths $\tilde{\lambda}_{m\alpha}$ depend on the population of the single-particle states and thus on the charge of the molecule. Specifically, an electron that is transferred from the electrode to the m th state of the *neutral* molecule couples with $\tilde{\lambda}_{m\alpha} = \lambda_{m\alpha}$ to the vibrational mode α . For an electron that populates state m of the *charged* molecule, where the occupation of the n th state differs from the neutral molecule, the effective electron-vibrational interaction is $\tilde{\lambda}_{m\alpha} = \lambda_{m\alpha} + W_{m\alpha}$. This implies the existence of different electronic-vibrational coupling strengths for the same electronic state, in the above example $\lambda_{m\alpha}$ and $\lambda_{m\alpha} + W_{m\alpha}$. The coupling strength relevant for an electron entering/leaving the molecule depends on the exact population of all the other electronic states at the very moment the transport process takes place. An interpretation based on an averaged electronic-vibrational coupling strength $\lambda_{m\alpha} + W_{m\alpha} \langle d_n^{\dagger} d_n - \delta_n \rangle$, therefore, does not provide a correct description of the physics. A quantitative description requires an explicit calculation of the transport characteristics, including vibrationally dependent electron-electron interactions, which will be the focus of Sec. III A.

C. Master equation approach

We simulate the transport properties of a single-molecule junction employing the well-established Born-Markov master

equation methodology [17,34,55,73–77]. Thereby, the central object is the reduced density matrix of the molecule ρ , which is obtained as the stationary solution of the equation of motion,

$$\partial_t \rho(t) = -i[\bar{H}_S, \rho(t)] - \int_0^{\infty} d\tau \text{tr}_B \{ [\bar{H}_{SB}, [\bar{H}_{SB}(\tau), \rho(t) \rho_B]] \}, \quad (21)$$

with

$$\bar{H}_{SB}(\tau) = e^{-i(\bar{H}_S + \bar{H}_B)\tau} \bar{H}_{SB} e^{i(\bar{H}_S + \bar{H}_B)\tau} \quad (22)$$

and ρ_B being the equilibrium density matrix of the leads. Equation (21) can be obtained, e.g., using a second-order expansion of the exact Nakajima-Zwanzig equation [78,79] in the coupling \bar{H}_{SB} , including the so-called Markov approximation. The expansion to second order in \bar{H}_{SB} allows for a description of all resonant transport processes, but it misses higher-order contributions such as cotunneling processes and the broadening of levels due to molecule-lead coupling. Therefore, we will restrict the study to systems with weak molecule-lead coupling. In the regime of strong molecule-lead coupling, vibrational effects are typically less pronounced because the time an electron spends on the molecule is short compared to the vibrational period.

We evaluate the master equation (21) for the steady state, focusing on model systems with two electronic states and a single vibrational mode, which is sufficient to show the generic effects of vibrationally dependent electron-electron interactions. In the calculations, we use basis functions $|n_1 n_2\rangle |v\rangle$ ($n_1, n_2 \in \{0, 1\}$) that represent the subspace of the electronic $|n_1 n_2\rangle$ and the vibrational degrees of freedom $|v\rangle$ ($v \in \mathbb{N}_0$) in occupation number representations, respectively. The coefficients of the reduced density matrix are thus denoted by

$$\begin{aligned} \rho_{n_1 n_2, n'_1 n'_2}^{vv'} &\equiv \langle n_1 n_2 | \rho^{vv'} | n'_1 n'_2 \rangle \\ &\equiv \langle n_1 n_2 | \langle v | \rho | v' \rangle | n'_1 n'_2 \rangle. \end{aligned} \quad (23)$$

The principal value terms in Eq. (21) describe the renormalization of the molecular energy levels due to the coupling between the bridge and the leads [34,75,80]. The importance of these terms has been investigated by Härtle and Millis in a recent study of charge-transfer dynamics in a double quantum dot system [80]. For the systems considered in this work, where the single-particle levels are well separated, these terms can be neglected. For the same reason, we neglect vibrational coherences in the density matrix, which is a valid assumption for the systems considered here, which do not exhibit quasidegeneracies and where the broadening due to molecule-lead coupling is small compared to the vibrational energies [34,81].

D. Observables of interest

To characterize electron transport through a single-molecule junction, we analyze the electric current and the average vibrational excitation as a function of applied bias voltage Φ .

Within the density matrix methodology outlined above, the expectation value of an observable O can be calculated as

$$\langle O \rangle = \text{tr} \{ \rho O \} = \sum_{n_1, n_2, v} \langle n_1 n_2 | \langle v | \rho O | v \rangle | n_1 n_2 \rangle. \quad (24)$$

TABLE I. Parameters of the model systems investigated in this article. For all calculations, the temperature is set to $T = 10$ K. All parameters are given in eV.

Model	ϵ_1	ϵ_2	ν_{L1}	ν_{R1}	ν_{L2}	ν_{R2}	β	Ω	λ_1	λ_2	U	\bar{U}	W
EFF*	0.15	0.3	0.1	0.1	0.1	0.1	3	0.1	0.05	0.05	0.7		$-0.1 \dots + 0.1$
EFF	0.15	0.3	0.1	0.1	0.1	0.1	3	0.1	0.05	0.05		0.525	$0, \pm 0.05$
STMSETUP	0.15	0.2	0.1	0.01	0.1	0.01	3	0.1	-0.05	0.05		1.05	$0, \pm 0.05$
DARKST	0.15	0.2	0.1	0.1	0.01	0.01	3	0.1	-0.05	0.05		0.05	$0, \pm 0.05$
ASYMM	0.15	0.3	0.1	0.03	0.1	0.03	3	0.1	0.05	0.05		0.525	$0, \pm 0.05$

Specifically, the excitation of the vibrational mode ν is given by [34]

$$\begin{aligned}
\langle a_\nu^\dagger a_\nu \rangle_H &= \langle a_\nu^\dagger a_\nu \rangle_{\bar{H}} + 2 \sum_{mn} \frac{\lambda_{m\nu} \lambda_{m\nu}}{\Omega_\nu^2} \langle (d_m^\dagger d_m - \delta_m)(d_n^\dagger d_n - \delta_n) \rangle_{\bar{H}} \\
&+ 2 \sum_{m,n < p} \frac{\lambda_{m\nu} W_{np\nu}}{\Omega_\nu^2} \langle (d_m^\dagger d_m - \delta_m)(d_n^\dagger d_n - \delta_n) \\
&\times (d_p^\dagger d_p - \delta_p) \rangle_{\bar{H}} + 2 \sum_{m < n, p < q} \frac{W_{m\nu} W_{pq\nu}}{\Omega_\nu^2} \langle (d_m^\dagger d_m - \delta_m) \\
&\times (d_n^\dagger d_n - \delta_n)(d_p^\dagger d_p - \delta_p)(d_q^\dagger d_q - \delta_q) \rangle_{\bar{H}}. \quad (25)
\end{aligned}$$

Thereby, the subscript H/\bar{H} denotes the Hamiltonian, which is used to evaluate the respective expectation value.

The number of electrons entering or leaving the lead K ($K \in \{L, R\}$) per unit time determines the electronic current,

$$\begin{aligned}
I_K &= \langle \hat{I}_K \rangle_H = -2e \frac{d}{dt} \sum_{k \in K} \langle c_k^\dagger c_k \rangle_{\bar{H}} \\
&= 2ie \left[\sum_{km} V_{mk} \langle c_k^\dagger d_m X_m \rangle_{\bar{H}} - \sum_{km} V_{mk}^* \langle d_m^\dagger X_m c_k \rangle_{\bar{H}} \right]. \quad (26)
\end{aligned}$$

Here, the constant ($-e$) denotes the electron charge, and the factor 2 accounts for spin degeneracy. To second order in the molecule-lead coupling, the current through lead K can be written as [55,73–75]

$$I_K \approx -i \int_0^\infty d\tau \text{tr}_{\text{S+B}} \{ [\bar{H}_{\text{SB}}(\tau), \rho_B \rho] \hat{I}_K \}. \quad (27)$$

It is noted that our scheme is current-conserving, i.e., $I_L = -I_R = I$.

III. RESULTS

To analyze the effect of vibrationally dependent electron-electron interactions, we consider a series of minimal models comprising two electronic levels and a single vibrational mode. The parameters of the models are summarized in Table I, where, for the sake of clarity, we dropped all vibrational indices and the electronic indices of U and W . The parameters characterizing the model systems represent typical values for molecular junctions, as known from experimental data [13,15,19,28,82–85] or first-principles-based calculations [40,57,59,86–88]. It is noted that all systems investigated exhibit relatively weak molecule-lead coupling strengths as imposed by the transport method used.

We start our study with an overview over the different effects and regimes associated with the vibrationally dependent electron-electron interaction strength W using the generic model EFF*. Subsequently, we exemplify the importance of the vibrationally dependent electron-electron interaction based on several distinct model systems that represent typical experimental setups. As such, models ASYMM and STM-SETUP exhibit a pronounced asymmetry with respect to the coupling to the left and right lead, as can be found in STM measurements. Finally, model DARKST describes molecules with one dominating conductance channel. Based on this model, we show the manifestation of vibrationally dependent electron-electron interactions as an effective population-dependent electronic-vibrational coupling and its influence on vibrational excitation. Furthermore, signatures of negative differential resistance and asymmetries in the gate voltage dependences of the current, even in symmetrically coupled molecular junctions, are analyzed.

A. Effective population-dependent electronic-vibrational coupling

We start the analysis of the influence of vibrationally dependent electron-electron interaction by studying the transport properties of the generic model system EFF* (see Table I) for varying interaction strengths W , thus giving a systematic overview over the influence of the W parameter. In this model, the electronic energy levels of the anion and the dianion are well separated, which allows for a better identification of the effect of vibrationally dependent electron-electron interaction.

Figure 2 shows the conductance $\frac{\partial I}{\partial V}$ of model EFF* as a function of bias voltage and vibrationally dependent electron-electron coupling strength W . Overall, the conductance exhibits straight vertical lines dominating the low bias regime and bend lines dominating the high bias and positive W regime. Furthermore, most of the lines in the high voltage regime of the conductance plot are disconnected in the region of $W = -0.05$ eV.

The straight lines in the conductance map correspond to the opening of electronic and vibronic transport channels that involve the anionic molecule. As these transport processes are not directly influenced by vibrationally dependent electron-electron interaction, the lines are unchanged upon variation of the coupling strength W . The bend lines, however, correspond to the opening of transport channels, where two additional electrons populate the molecule during the transport processes. These transport channels are directly influenced by the coupling strength W . The shape of the lines is described by Eq. (18). In the following, we analyze the conductance in more

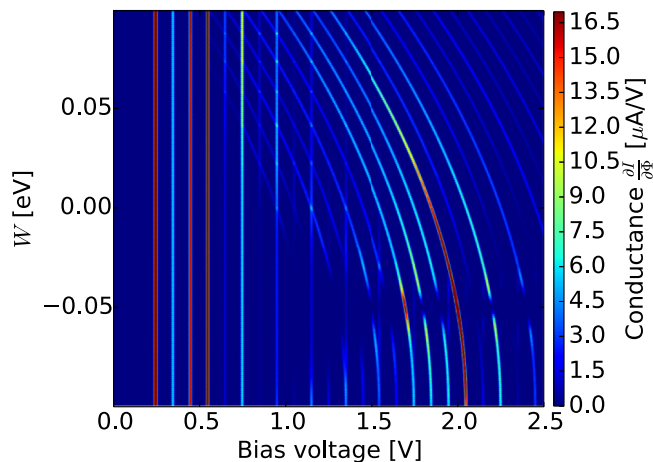


FIG. 2. Conductance of model system EFF* as a function of bias voltage and vibrationally coupled electron-electron coupling strength W .

detail for two values of the electron-electron coupling strength, $W = \pm 0.05$ eV, corresponding to two different transport regimes.

Figure 3 shows the current and the vibrational excitation as a function of bias voltage Φ for model system EFF for $W = \pm 0.05$ eV. Model EFF is identical to model EFF* apart from the fact that, for better comparison, the value of \bar{U} is fixed and the bare Coulomb interaction strength U is adjusted such that the location of the electronic resonances coincides for all values of W . As a reference, data obtained without vibrationally dependent electron-electron interaction, i.e., $W = 0$ eV, are also depicted. The results show that the vibrationally dependent electron-electron interaction has a significant effect for voltages $\Phi > 2\bar{\epsilon}_2$. Depending on the sign of the interaction W and the specific voltage, it results in a decrease or increase of the current compared to the system without interaction. Moreover, vibrational excitation is enhanced for $W = -0.05$ eV and reduced for $W = 0.05$ eV.

These findings can be explained employing the effective electronic-vibrational coupling strength $\tilde{\lambda}_i$ introduced in Eq. (20). We start by considering the case $W = +0.05$ eV. For low bias voltages, $\Phi \ll 2(\bar{\epsilon}_1 + \bar{U})$, the current and the vibrational excitation agree with the noninteracting model. At these voltages, the features in the current-voltage and vibrational excitation characteristics are related to the opening of transport channels at energies $\bar{\epsilon}_{1/2} + m\Omega$ with $m \in \mathbb{Z}$. Populating both electronic states, $\bar{\epsilon}_1$ and $\bar{\epsilon}_2$, is not possible at these low voltages because the electrons coming from the leads do not have enough energy to overcome the Coulomb repulsion. Accordingly, an electron impinging on the molecular bridge from the left electrode encounters a neutral molecule. Therefore, in this elementary charge transport step, the electron couples to the vibrational degrees of freedom with the coupling strengths $\tilde{\lambda}_i = \lambda_i + W \times 0 = \lambda_i$, which is independent of the vibrationally dependent electron-electron interaction W . As a consequence, the transport properties at low voltages are basically identical to those of the system without the vibrationally dependent electron-electron interaction.

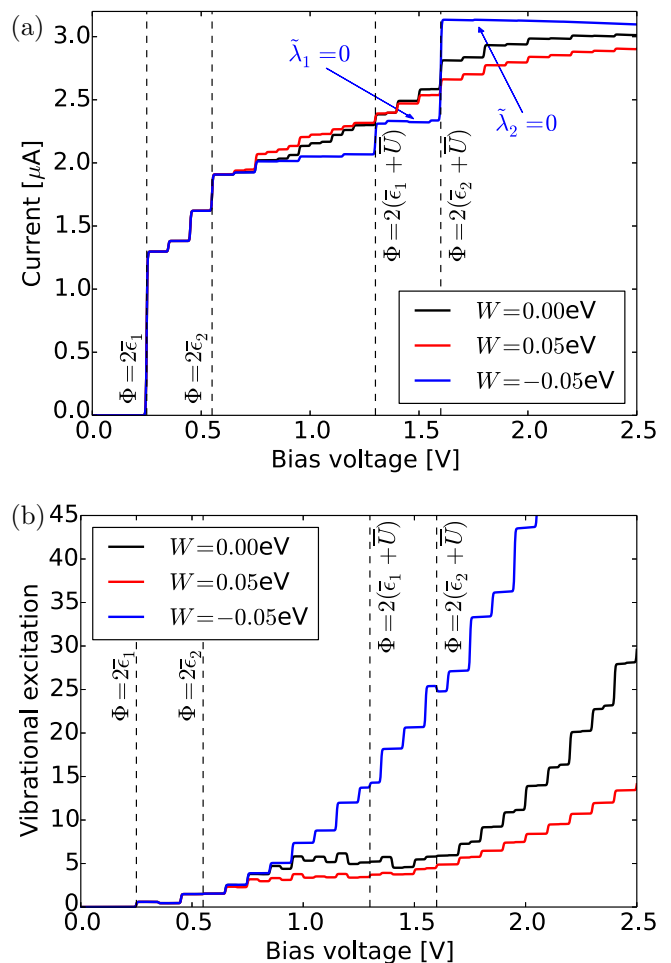


FIG. 3. (a) Current-voltage characteristics for the model system EFF. (b) Vibrational excitation as a function of bias voltage for the system EFF. The vertical dashed lines in both plots mark the onset of resonant transport through the corresponding molecular electronic states.

For higher voltages, $\Phi \gtrsim 2(\bar{\epsilon}_1 + \bar{U})$, new features in the current and the vibrational excitation characteristics appear that are associated with the opening of transport channels at energies $\bar{\epsilon}_{1/2} + \bar{U} + m\Omega$ with $m \in \mathbb{Z}$ and correspond to transport channels where the electron impinging from the left electrode onto the molecule encounters a singly occupied molecular bridge. As a consequence, in the elementary charge transport steps, the electron couples to the vibrational degrees of freedom $\tilde{\lambda}_i = \lambda_i + W \times 1 = \lambda_i + W$. For $W = +0.05$ eV, the effective electronic-vibrational coupling is thus increased, which leads to two effects observed in Fig. 3: First, resonant transport processes associated with the absorption of vibrational energy are enhanced, resulting in an increased current for voltages below the onset of resonant transport involving the dianionic molecule, $\Phi < 2(\bar{\epsilon}_2 + \bar{U})$ [17,34]. These processes also lead to a decreased vibrational excitation seen in the corresponding voltage regime in Fig. 3(b). Second, in the weak electronic-vibrational coupling regime considered here, an increased electronic-vibrational interaction gives rise to a decreased current and a diminished vibrational excitation beyond the onset of resonant transport involving the respective

electronic state [17,34,89–91], in this case the dianionic resonance, at voltages $\Phi > 2(\bar{\epsilon}_2 + \bar{U})$.

It is important to note that the current at these higher voltages includes both transport channels that couple with $\tilde{\lambda}_i = \lambda_i$ to the vibrations and which became active already at low bias voltages, and transport channels that couple with $\tilde{\lambda}_i = \lambda_i + W$. Although the average populations of the two electronic levels saturate at about $\langle d_1^\dagger d_1 \rangle \approx \langle d_2^\dagger d_2 \rangle \approx 0.5$ at high bias voltages, we want to stress that the above-discussed transport behavior is not described correctly by considering transport with electronic-vibrational coupling strengths of $\tilde{\lambda}_i = \lambda_i + W \times 0.5$ corresponding to the average population, but we must consider the populations of the elementary charge transport steps, which are 0 or 1, as discussed above.

Next we consider the system with $W = -0.05$ eV. For low voltages, as discussed above, the transport is determined by the effective coupling $\tilde{\lambda}_i = \lambda_i + W \times 0$ and thus independent of W . At higher voltages, $\Phi \gtrsim 2(\bar{\epsilon}_1 + \bar{U})$, however, the features in the current and the vibrational excitation are associated predominantly with transport processes, where an electron coming from the left electrode encounters a singly occupied molecular bridge resulting in an effective coupling of $\tilde{\lambda}_i = \lambda_i + W \times 1 = 0$ eV for the chosen parameters of the model, $\lambda = -W = 0.05$ eV. This corresponds to a system in which the electronic-vibrational coupling and the vibrationally dependent electron-electron interaction cancel each other. Compared to the system with $W = 0$ eV, this results in a smaller current for $2\bar{\epsilon}_1 < e\Phi < 2(\bar{\epsilon}_1 + \bar{U})$ and a larger current for $e\Phi > 2(\bar{\epsilon}_2 + \bar{U})$. At higher bias voltages, the Franck-Condon blockade of the current is lifted, while the smaller current at lower voltages is due to the absence of transport processes associated with the absorption of vibrational energy. This is also reflected in the vibrational excitation characteristics [Fig. 3(b)], which for $W = -0.05$ eV exhibits a steady increase with voltage indicating the absence of processes that absorb vibrational energy. This increase of vibrational excitation is further enhanced because decreased electronic-vibrational coupling leads to increased vibrational excitation in the regime of weak electronic-vibrational coupling due to missing electron-hole pair creation processes that effectively cool the molecular bridge [92]. As a result, the largest average vibrational excitation is observed for the system $W = -0.05$ eV. Notice that the vanishing effective electronic-vibrational coupling $\tilde{\lambda}_i = 0$ eV also explains the disconnected lines in Fig. 2 at high bias voltages close to $W = -0.05$ eV.

To conclude this section, we comment on the validity of the adiabatic approximation employed in our model Hamiltonian Eq. (5). As shown in our previous study [26], nonadiabatic effects in transport become important if the energy difference of the electronic states $\bar{\epsilon}_2 - \bar{\epsilon}_1$ is close to a multiple of the vibrational frequency Ω . In system EFF^(*) and all other models considered in this paper, $\bar{\epsilon}_2 - \bar{\epsilon}_1$ differs from Ω by more than the broadening caused by the coupling to the leads. Thus, the adiabatic approximation is valid. Notice that \bar{U} is irrelevant for this consideration, as an electron must have the possibility to scatter from one state to the other. Consequently, there must be at least one unoccupied electronic state. For Fig. 2, this means that even at the points of intersections, the nonadiabatic electronic-vibrational interaction would not play an important role, as the bend lines are associated with doubly occupied

electronic states, whereas the straight lines correspond to anionic states.

B. Effect of vibrationally dependent electron-electron interactions in molecular junctions with left-right asymmetry

The additional effect of vibrationally dependent electron-electron interactions arises in models with asymmetric coupling to left and right leads, as is common, e.g., in STM setups. As an example, we consider the model system STMSETUP with parameters listed in Table I. Due to the difference in the coupling to the leads, the electronic states of the molecular bridge are completely occupied for positive bias voltages above the onset of resonant transport through the respective levels. For negative bias voltages, they are unoccupied. The anionic molecule can be in its electronic ground ($\bar{\epsilon}_1$ occupied, $\bar{\epsilon}_2$ unoccupied) or first excited state ($\bar{\epsilon}_1$ unoccupied, $\bar{\epsilon}_2$ occupied). Depending on the electronic configuration of the anion, the dianion is obtained by populating the first or the second electronic state. For the specific choice of the parameters, $\lambda_1 = -\lambda_2 = \pm W$, one of these channels for generating the dianion decouples from the vibrations ($\tilde{\lambda}_1 = 0$ eV or $\tilde{\lambda}_2 = 0$ eV; see below). This allows for a better identification of the effect of vibrationally dependent electron-electron interaction in the current and vibrational excitation characteristics.

The current-voltage characteristics of model STMSETUP, depicted in Fig. 4(a), exhibit a pronounced asymmetry with respect to bias polarity, which is a well-known effect associated with the asymmetric coupling to the leads and the resulting dependence of the electronic population on bias polarity [34], but barely vary with W . However, as shown in Fig. 4(b), there is a significant influence of the vibrationally dependent electron-electron interaction on the vibrational excitation for positive bias voltage. Two features are noteworthy: First, for $W \neq 0$ eV, there is a sudden decrease in vibrational excitation at voltages $\Phi = 2(\bar{\epsilon}_{1/2} + \bar{U})$, where the dianion becomes energetically accessible [see the inset of Fig. 4(b)]. Second, for high bias voltages, the vibrational excitation is significantly smaller compared to the $W = 0$ case, independent of the sign of W .

These findings can be explained considering the population of the electronic states and the effective electronic-vibrational couplings $\tilde{\lambda}_i$. Due to the asymmetric coupling to the leads, the molecule is mostly in the dianionic state, once the applied positive bias allows for double charging of the molecule. As a consequence, electrons populating the molecule from the left encounter an anionic molecule most of the time, and transport processes with coupling $\tilde{\lambda}_{1/2} = \tilde{\lambda}_{1/2} + W \times 1$ to the vibrational degrees of freedom are dominant. Because one of the effective couplings vanishes ($\tilde{\lambda}_1 = 0$ eV or $\tilde{\lambda}_2 = 0$ eV), the average vibrational excitation strongly decreases at the bias voltage where transport with $\tilde{\lambda}_{1/2} = 0$ eV becomes energetically possible.

For large positive bias voltages, beyond the onset of transport involving the dianion, both molecular electronic states are almost always occupied. Accordingly, the current flowing across the molecule in this bias regime is determined by the transport processes that rely on the generation of the dianion. For the system without vibrationally dependent electron-electron interaction, the transport through both

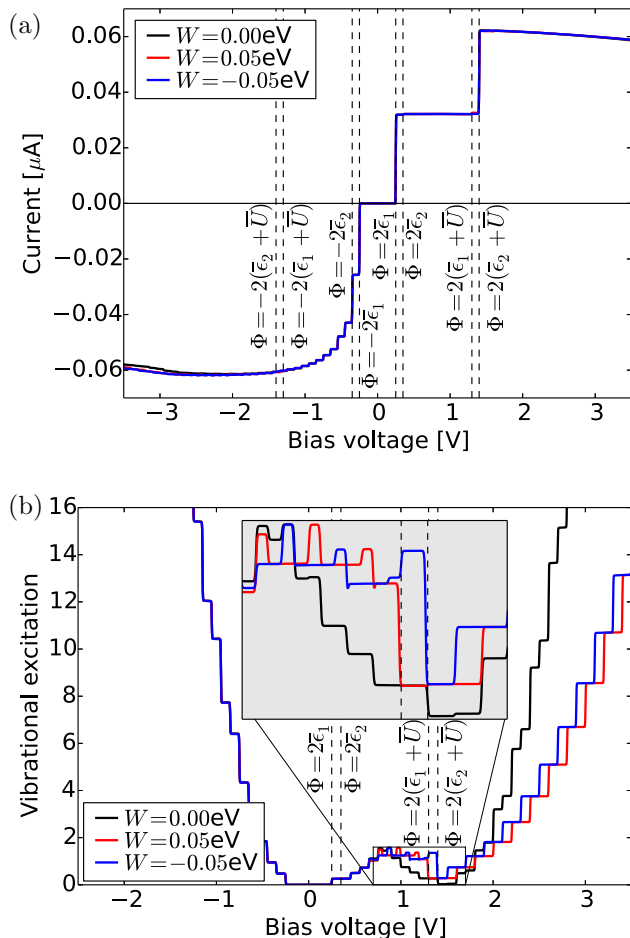


FIG. 4. (a) Current-voltage characteristics for the model system STMSETUP. (b) Vibrational excitation as a function of bias voltage for the system STMSETUP. The vertical dashed lines in both plots mark the onset of resonant transport through the corresponding molecular electronic states. The inset in panel (b) shows an enlargement of the region $\Phi \approx 2(\bar{\epsilon}_{1/2} + \bar{U})$.

electronic states couples with λ to the nuclear degrees of freedom. Thus both transport channels cause a heating of the vibrational mode. For the systems with $W \neq 0$ eV, on the other hand, only the transport channel through one of the electronic states couples to the vibrations with twice the coupling strength, 2λ , whereas the other decouples from the vibrations. As a stronger electronic-vibrational coupling leads to a decreased vibrational excitation in the regime of overall weak electronic-vibrational coupling (i.e., $\lambda < \Omega$) [17,34], the systems with $W = \pm 0.05$ eV exhibit on average a smaller number of vibrational quanta for large positive bias voltages.

C. Negative differential resistance

Another effect introduced by vibrationally dependent electron-electron interaction is negative differential resistance (NDR), which is a decrease in current upon an increase of bias voltage. To demonstrate this effect, we consider the model system DARKST as specified in Table I. It consists of a strongly coupled electronic state $\bar{\epsilon}_1$, which is mainly responsible for the current flowing through the molecule, and

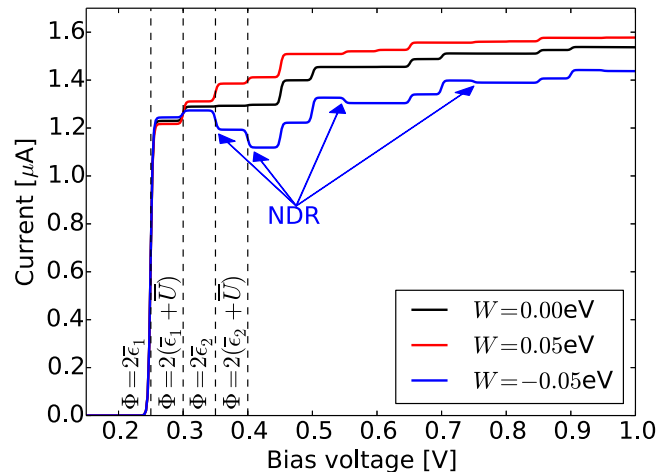


FIG. 5. Current-voltage characteristics of model system DARKST. The vertical dashed lines mark the onset of resonant transport through molecular electronic states.

a weaker coupled or dark state $\bar{\epsilon}_2$, which mainly influences the transport properties of the main channel via vibrationally dependent electron-electron interaction. Again, the electron-electron interaction has been adapted such that the location of the electronic resonances coincides for the systems with $W = 0, \pm 0.05$ eV.

The current-voltage characteristics for the model system, depicted in Fig. 5, exhibit one large step at $\Phi = 2\bar{\epsilon}_1$, marking the onset of resonant transport through $\bar{\epsilon}_1$, and additional, smaller vibrational features, which depend on the magnitude and sign of W . The influence of the second transport channel $\bar{\epsilon}_2$ is barely visible due to its weak coupling to the leads. For the case $W = 0$, the main steps of the current are at $\Phi = 2(\bar{\epsilon}_1 + n\Omega)$ and $\Phi = 2(\bar{\epsilon}_1 + \bar{U} + n\Omega)$ with $n \in \mathbb{N}_0$. For $W = \pm 0.05$ eV, however, there are also distinct features at $\Phi = 2(\bar{\epsilon}_2 + n\Omega)$ and $\Phi = 2(\bar{\epsilon}_2 + \bar{U} + n\Omega)$. While for $W = 0.05$ eV the current is overall larger than for the reference system $W = 0$, for $W = -0.05$ eV it is reduced. Furthermore, for $W = -0.05$ eV, the vibrational features give rise to distinct decreases in the current upon increasing bias voltage. This NDR effect is marked by blue arrows in Fig. 5.

We first consider the results for $W = 0.05$ eV. In this case, the effective couplings for transport through level $\bar{\epsilon}_1$ are $\tilde{\lambda}_1 = -0.05$ eV and $\tilde{\lambda}_1 = -0.05$ eV + $W = 0$ eV, respectively, depending on the occupation of the levels. For transport through level $\bar{\epsilon}_2$, the effective electronic-vibrational couplings are $\tilde{\lambda}_2 = 0.05$ eV and $\tilde{\lambda}_2 = 0.05$ eV + $W = 0.1$ eV. Notice that the latter corresponds to an enhanced coupling for transport involving the dianion. With the population of $\bar{\epsilon}_2$ at biases $\Phi > 2\bar{\epsilon}_2$, the current flowing through $\bar{\epsilon}_1$ comprises transport channels that involve the dianion. As this transport path decouples from the vibrations, $\tilde{\lambda}_1 = 0$ eV, the current is increased compared to transport through $\bar{\epsilon}_1$ of the anionic molecule with $\tilde{\lambda}_1 = -0.05$ eV.

Next we study the current-voltage characteristics for $W = -0.05$ eV. In this case, the effective electronic-vibrational couplings for level $\bar{\epsilon}_1$ are $\tilde{\lambda}_1 = -0.05$ eV and $\tilde{\lambda}_1 = -0.05$ eV + $W = -0.1$ eV. Notice that transport

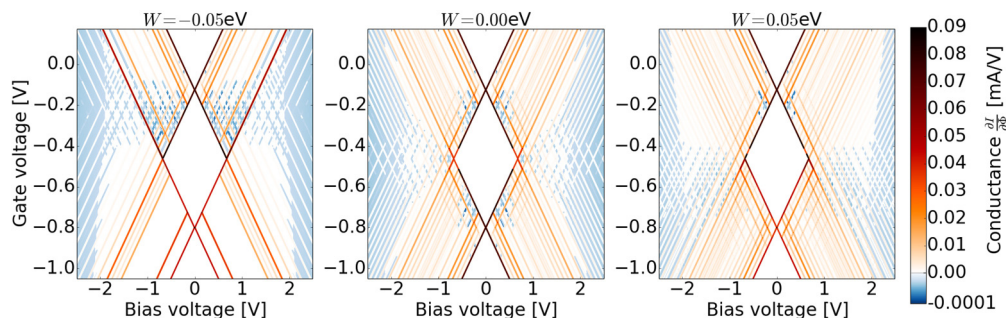


FIG. 6. Conductance as a function of bias and gate voltage for the system EFF for $W = 0, \pm 0.05$ eV. Notice the different scale used for negative conductances.

through $\bar{\epsilon}_1$ involving the dianion corresponds to an enhanced electronic-vibrational coupling. For transport through level $\bar{\epsilon}_2$, the effective electronic-vibrational couplings are $\tilde{\lambda}_2 = 0.05$ eV and $\tilde{\lambda}_2 = 0.05$ eV + $W = 0$ eV. For $\Phi = 2(\bar{\epsilon}_1 + n\Omega)$ and $\Phi = 2(\bar{\epsilon}_1 + \bar{U} + n\Omega)$, we observe an increase in the current that is associated with the opening of new transport channels directly populating $\bar{\epsilon}_1$. For $\Phi = 2(\bar{\epsilon}_2 + n\Omega)$ and $\Phi = 2(\bar{\epsilon}_2 + \bar{U} + n\Omega)$, on the other hand, new transport channels directly populating level $\bar{\epsilon}_2$ become available. Consequently, transport processes involving the dianionic molecule become more important, thus increasing the significance of transport through $\bar{\epsilon}_1$ with enhanced electronic-vibrational coupling strength $\tilde{\lambda}_1 = -0.1$ eV. As the transport through $\bar{\epsilon}_1$ dominates the current, and an enhanced electronic-vibrational coupling results in a smaller current, a stepwise decrease of the current is observed at bias voltages $\Phi = 2(\bar{\epsilon}_2 + n\Omega)$ and $\Phi = 2(\bar{\epsilon}_2 + \bar{U} + n\Omega)$. Notice that this NDR effect results from the influence of the level $\bar{\epsilon}_2$ on the transport through $\bar{\epsilon}_1$ via the population-dependent electronic-vibrational coupling $\tilde{\lambda}_1$. The NDR effect is therefore qualitatively different from similar NDR effects such as blocking state scenarios [34].

It is important to emphasize that there are model systems in which the renormalization of the electron-electron interaction strength $U \rightarrow \bar{U}$ caused by the vibrationally dependent electron-electron interaction can also result in NDR. However, this effect does not appear in the model DARKST considered above.

D. Asymmetries with respect to bias and gate voltage

The vibrationally dependent electron-electron interaction leads to vibrational effects that are influenced by the electronic population of the molecular levels. As a consequence, vibrational features can change with bias polarity and gate voltage. In this section, we study these dependences based on conductance maps, that is, the conductance as a function of bias and gate voltage. Thereby, we assume that the only effect of a gate voltage Φ_{gate} on the system is to shift the electronic energies of the noninteracting molecule, $\epsilon_i \rightarrow \epsilon_i + \Phi_{\text{gate}}$ [93]. Other investigations of molecular junction transport based on conductance maps, also referred to as Coulomb diamonds or stability diagrams, can be found, e.g., in [6,11,91,93–99].

We start with model system EFF from Sec. III A, which is characterized by a symmetric coupling to the leads and

vibrations. Figure 6 shows the conductance for coupling strengths of $W = 0, \pm 0.05$ eV. The conductance maps are dominated by the darker red lines, forming a diamond-shaped square in the center. These lines correspond to the onset of resonant transport through the electronic levels. Since the systems are corrected for the energy shift introduced by the vibrationally dependent electron-electron interaction, these features appear at the same positions for any value of W . Additionally, the conductance maps exhibit a distinct structure of less pronounced lines, which are associated with the onset of vibrationally dependent transport and differ in magnitude with W . For $W = -0.05$ eV, fewer vibrational lines are visible, and for $W = +0.05$ eV, the vibrational structures are observed over a wider range of voltages compared to the $W = 0$ eV case. For $W = 0$ eV, the conductance maps exhibits three symmetries with respect to the transformations $\Phi_{\text{bias}} \rightarrow -\Phi_{\text{bias}}, \Phi_{\text{gate}} \rightarrow -\Phi_{\text{gate}} - (\bar{\epsilon}_1 + \bar{\epsilon}_2 + \bar{U})$ and consequently also with respect to $\Phi_{\text{bias}}, \Phi_{\text{gate}} \rightarrow -\Phi_{\text{bias}}, -\Phi_{\text{gate}} - (\bar{\epsilon}_1 + \bar{\epsilon}_2 + \bar{U})$. The first is due to the symmetric coupling of the molecule to the leads and is unaffected by the vibrationally dependent electron-electron interaction. The second and third symmetry are broken for $W \neq 0$ eV. Lastly, the data show blue patterns, corresponding to small negative differential resistance, located at high bias voltages but also in areas close to the onset of resonant transport.

These findings can be rationalized as follows. The location of the lines related to electronic and vibronic transport is unchanged by W because the vibrationally dependent electron-electron interaction does not alter the vibrational energy. For $W = -0.05$ eV, fewer vibrational transport channels exist as transport involving the dianionic resonance effectively decouples from the nuclear degrees of freedom. For $W = +0.05$ eV, transport including the dianionic molecule couples with twice the strength to the nuclear displacement such that processes including several vibrational quanta are more pronounced than in the $W = 0$ eV case. The symmetry with respect to the gate voltage is lifted because the vibrational effects depend on the electronic population of the molecule. This leads to a change of the effective electronic-vibrational coupling upon variation in gate voltage, and hence to a different vibrational structure. The origin of the NDR for high bias voltages is the finite bandwidth of the leads, which are modeled as semi-infinite chains. The NDR for the model system with $W = 0.00$ eV for gate voltages around $-0.2, -0.475$, and -0.7 V is caused

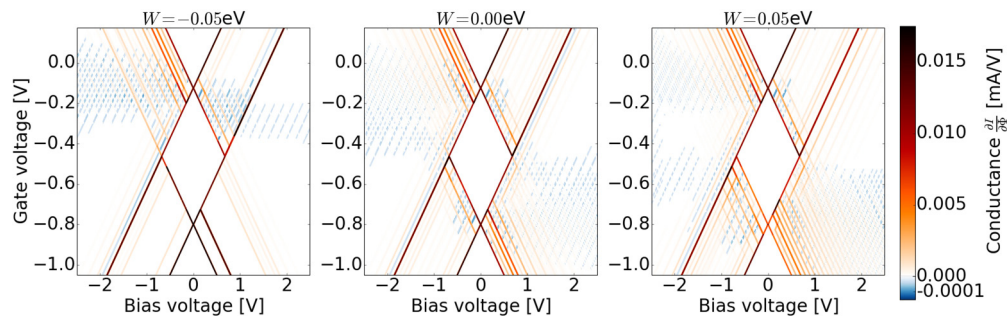


FIG. 7. Conductance as a function of bias and gate voltage for the system ASYMM for $W = 0, \pm 0.05$ eV. Notice the different scaling for negative conductances.

by the influence of the vibrational nonequilibrium state on the transport properties of the junction, as discussed in Ref. [34]. The change in the NDR structure for $W \neq 0$ eV is related to the change in the effective electronic-vibrational coupling for transport involving the dianion, resulting in an altered vibrational nonequilibrium state and the effect discussed in Sec. III C.

Next, we consider the model system ASYMM with asymmetric molecule-lead coupling, which allows us to study the relation between the vibrationally dependent electron-electron interaction and bias polarity. The corresponding conductance maps for $W = 0, \pm 0.05$ eV are shown in Fig. 7. As a consequence of its asymmetric coupling to the leads, the electronic population of this model is sensitive to the polarity of the applied bias, and so is the influence of the vibrationally dependent electron-electron interaction. As in the previous model, we observe a change in the vibrational structure of the conductance map upon a variation in W . For $W = -0.05$ eV, the lines corresponding to vibrational transport are less pronounced. In particular, for gate voltages below ≈ -0.45 V only few vibrational features are present. For $W = +0.05$ eV, the vibrational features are more pronounced and are observed for all gate voltages. The data also exhibit weak NDR effects, which are influenced by the vibrationally dependent electron-electron interaction. Due to the asymmetric coupling to the leads, there is no symmetry in the conductance maps with respect to bias polarity, $\Phi_{\text{bias}} \rightarrow -\Phi_{\text{bias}}$. Remarkably, also the symmetry of the conductance map under the transformation $\Phi_{\text{bias}}, \Phi_{\text{gate}} \rightarrow -\Phi_{\text{bias}}, -\Phi_{\text{gate}} - (\bar{\epsilon}_1 + \bar{\epsilon}_2 + \bar{U})$ is broken for $W \neq 0$. In the $W = 0$ eV case, this symmetry is a consequence of the fact that both the bias and gate voltage change the average population of the electronic states in a similar way and that there is no distinction between transport involving the anion or the dianion. Including vibrationally dependent electron-electron interaction, transport involving the anion or the dianion is no longer equivalent. As a result, the transport mechanism depends on the total charge of the molecule, and therefore this symmetry of the conductance map is broken. It is interesting to note that most of the conductance maps measured in experiment display similar asymmetries [6,11,94–96].

IV. CONCLUSION

We have investigated the effect of vibrationally dependent electron-electron interaction in single-molecule junctions.

The additional interaction is a result of the dependence of the Coulomb interaction on the nuclear displacement, and it accounts for the fact that vibronic transport processes depend on the charge state of the molecule, i.e., they are different for transport through, e.g., an anionic or dianionic state of the molecule. Employing a generalized small polaron transform, we have shown that vibrationally dependent electron-electron interaction results in an effective electronic-vibrational coupling, which depends on the electronic occupation and can be used to rationalize the effects on charge transport.

Employing a master equation approach, we have analyzed the basic mechanism and the manifestations of vibrationally dependent electron-electron interactions in single-molecule junctions. Depending on the strength and the sign of the interaction, it may result in significant, qualitative changes in the transport characteristics and the vibrational nonequilibrium excitation and may cause NDR. For selected values of the interaction strength, the interplay between electronic-vibrational interaction and vibrationally dependent electron-electron interaction can also lead to regimes where electronic-vibrational coupling is effectively switched off. In junctions with asymmetric molecule-lead coupling, vibrationally dependent electron-electron interaction may cause a strong dependence of the vibrational nonequilibrium excitation on the bias polarity. Finally, vibrationally dependent electron-electron interaction can give rise to asymmetries of conductance maps related to the different mechanisms of transport involving the anionic and the dianionic molecule. The latter finding may be of particular interest in the context of experimental results, which have the tendency to display asymmetries [6,11,94–96].

ACKNOWLEDGMENTS

We thank C. Schinabeck and P. B. Coto for helpful discussions. This work has been supported by the German-Israeli Foundation for Scientific Development (GIF) and the Deutsche Forschungsgemeinschaft (DFG) through the DFG-Cluster of Excellence ‘Engineering of Advanced Materials’, SFB 953, and a research grant. The generous allocation of computing time by the computing centers in Erlangen (RRZE) and Munich (LRZ) is gratefully acknowledged. RH was supported by the Alexander von Humboldt foundation via a Feodor-Lynen research fellowship.

- [1] M. Galperin, M. A. Ratner, and A. Nitzan, *J. Phys.: Condens. Matter* **19**, 103201 (2007).
- [2] S. W. Wu, G. V. Nazin, X. Chen, X. H. Qiu, and W. Ho, *Phys. Rev. Lett.* **93**, 236802 (2004).
- [3] B. J. LeRoy, S. G. Lemay, J. Kong, and C. Dekker, *Nature (London)* **432**, 371 (2004).
- [4] L. H. Yu, Z. K. Keane, J. W. Ciszek, L. Cheng, M. P. Stewart, J. M. Tour, and D. Natelson, *Phys. Rev. Lett.* **93**, 266802 (2004).
- [5] A. N. Pasupathy, J. Park, C. Chang, A. V. Soldatov, S. Lebedkin, R. C. Bialczak, J. E. Grose, L. A. K. Donev, J. P. Sethna, D. C. Ralph, and P. L. McEuen, *Nano Lett.* **5**, 203 (2005).
- [6] S. Sapmaz, P. Jarillo-Herrero, Y. M. Blanter, C. Dekker, and H. S. J. van der Zant, *Phys. Rev. Lett.* **96**, 026801 (2006).
- [7] W. H. A. Thijssen, D. Djukic, A. F. Otte, R. H. Bremmer, and J. M. van Ruitenbeek, *Phys. Rev. Lett.* **97**, 226806 (2006).
- [8] J. J. Parks, A. R. Champagne, G. R. Hutchison, S. Flores-Torres, H. D. Abruna, and D. C. Ralph, *Phys. Rev. Lett.* **99**, 026601 (2007).
- [9] T. Böhler, A. Edtbauer, and E. Scheer, *Phys. Rev. B* **76**, 125432 (2007).
- [10] N. P. de Leon, W. Liang, Q. Gu, and H. Park, *Nano Lett.* **8**, 2963 (2008).
- [11] A. K. Hüttel, B. Witkamp, M. Leijnse, M. R. Wegewijs, and H. S. J. van der Zant, *Phys. Rev. Lett.* **102**, 225501 (2009).
- [12] J. Hihath, C. Bruot, and N. Tao, *ACS Nano* **4**, 3823 (2010).
- [13] S. Ballmann, W. Hieringer, D. Secker, Q. Zheng, J. A. Gladysz, A. Görling, and H. B. Weber, *Chem. Phys. Chem.* **11**, 2256 (2010).
- [14] A. D. Jewell, H. L. Tierney, A. E. Baber, E. V. Iski, M. M. Laha, and E. C. H. Sykes, *J. Phys.: Condens. Matter* **22**, 264006 (2010).
- [15] E. A. Osorio, M. Ruben, J. S. Seldenthuis, J. M. Lehn, and H. S. J. van der Zant, *Small* **6**, 174 (2010).
- [16] J. Koch and F. von Oppen, *Phys. Rev. Lett.* **94**, 206804 (2005).
- [17] R. Härtle, C. Benesch, and M. Thoss, *Phys. Rev. Lett.* **102**, 146801 (2009).
- [18] G. Romano, A. Gagliardi, A. Pecchia, and A. Di Carlo, *Phys. Rev. B* **81**, 115438 (2010).
- [19] D. Secker, S. Wagner, S. Ballmann, R. Härtle, M. Thoss, and H. B. Weber, *Phys. Rev. Lett.* **106**, 136807 (2011).
- [20] R. Volkovich, R. Härtle, M. Thoss, and U. Peskin, *Phys. Chem. Chem. Phys.* **13**, 14333 (2011).
- [21] S. Ballmann, W. Hieringer, R. Härtle, P. B. Coto, M. R. Bryce, A. Görling, M. Thoss, and H. B. Weber, *Phys. Status Solidi B* **250**, 2452 (2013).
- [22] R. Härtle, U. Peskin, and M. Thoss, *Phys. Status Solidi B* **250**, 2365 (2013).
- [23] A. S. Martin and J. R. Sambles, *Nanotechnology* **7**, 401 (1996).
- [24] M. Galperin, A. Nitzan, M. A. Ratner, and D. R. Stewart, *J. Phys. Chem. B* **109**, 8519 (2005).
- [25] I. Diez-Perez, J. Hihath, Y. Lee, L. Yu, L. Adamska, M. A. Kozhushner, I. I. Oleynik and N. Tao, *Nat. Chem.* **1**, 635 (2009).
- [26] A. Erpenbeck, R. Härtle, and M. Thoss, *Phys. Rev. B* **91**, 195418 (2015).
- [27] R. Härtle, M. Butzin, O. Rubio-Pons, and M. Thoss, *Phys. Rev. Lett.* **107**, 046802 (2011).
- [28] S. Ballmann, R. Härtle, P. B. Coto, M. Elbing, M. Mayor, M. R. Bryce, M. Thoss, and H. B. Weber, *Phys. Rev. Lett.* **109**, 056801 (2012).
- [29] R. Härtle, M. Butzin, and M. Thoss, *Phys. Rev. B* **87**, 085422 (2013).
- [30] D. Boese and H. Schoeller, *Europhys. Lett.* **54**, 668 (2001).
- [31] J. Koch and F. von Oppen, *Phys. Rev. B* **72**, 113308 (2005).
- [32] A. Zazunov, D. Feinberg, and T. Martin, *Phys. Rev. B* **73**, 115405 (2006).
- [33] M. Leijnse and M. R. Wegewijs, *Phys. Rev. B* **78**, 235424 (2008).
- [34] R. Härtle and M. Thoss, *Phys. Rev. B* **83**, 115414 (2011).
- [35] M. Galperin, M. A. Ratner, and A. Nitzan, *Nano Lett.* **5**, 125 (2005).
- [36] K. F. Albrecht, H. Wang, L. Mühlbacher, M. Thoss, and A. Komnik, *Phys. Rev. B* **86**, 081412 (2012).
- [37] K. F. Albrecht, A. Martin-Rodero, R. C. Monreal, L. Mühlbacher, and A. Levy Yeyati, *Phys. Rev. B* **87**, 085127 (2013).
- [38] E. Y. Wilner, H. Wang, M. Thoss, and E. Rabani, *Phys. Rev. B* **89**, 205129 (2014).
- [39] L. S. Cederbaum and W. Domcke, *J. Chem. Phys.* **60**, 2878 (1974).
- [40] C. Benesch, M. Cizek, J. Klimes, M. Thoss, and W. Domcke, *J. Phys. Chem. C* **112**, 9880 (2008).
- [41] J. E. Han, *Phys. Rev. B* **81**, 113106 (2010).
- [42] M. Cizek, M. Thoss, and W. Domcke, *Czech. J. Phys.* **55**, 189 (2005).
- [43] A. Donarini, M. Grifoni, and K. Richter, *Phys. Rev. Lett.* **97**, 166801 (2006).
- [44] H. Hübener and T. Brandes, *Phys. Rev. Lett.* **99**, 247206 (2007).
- [45] F. Elste and F. von Oppen, *New J. Phys.* **10**, 065021 (2008).
- [46] I. A. Pshenichnyuk and M. Čížek, *Phys. Rev. B* **83**, 165446 (2011).
- [47] J. Brüggemann, G. Weick, F. Pistolesi, and F. von Oppen, *Phys. Rev. B* **85**, 125441 (2012).
- [48] L. Simine and D. Segal, *J. Chem. Phys.* **141**, 014704 (2014).
- [49] R. van Leeuwen, *Phys. Rev. B* **69**, 115110 (2004).
- [50] T. G. Schmalz, L. Serrano-Andrés, V. Sauri, M. Merchán, and J. M. Oliva, *J. Chem. Phys.* **135**, 194103 (2011).
- [51] A. A. Dzhoiev, D. S. Kosov, and F. von Oppen, *J. Chem. Phys.* **138**, 134103 (2013).
- [52] R. Pozner, E. Lifshitz, and U. Peskin, *Nano Lett.* **14**, 6244 (2014).
- [53] V. Garca, R. Caballol, and J. Malrieu, *Chem. Phys. Lett.* **261**, 98 (1996).
- [54] S. Braig and K. Flensberg, *Phys. Rev. B* **68**, 205324 (2003).
- [55] A. Mitra, I. Aleiner, and A. J. Millis, *Phys. Rev. B* **69**, 245302 (2004).
- [56] L. S. Cederbaum and W. Domcke, *J. Chem. Phys.* **64**, 603 (1976).
- [57] C. Benesch, M. Cizek, M. Thoss, and W. Domcke, *Chem. Phys. Lett.* **430**, 355 (2006).
- [58] I. Kondov, M. Cizek, C. Benesch, M. Thoss, and H. Wang, *J. Phys. Chem. C* **111**, 11970 (2007).
- [59] C. Benesch, M. F. Rode, M. Cizek, R. Härtle, O. Rubio-Pons, M. Thoss, and A. L. Sobolewski, *J. Phys. Chem. C* **113**, 10315 (2009).
- [60] R. Härtle, Ph.D. thesis, Friedrich-Alexander-Universität Erlangen-Nürnberg (2012).
- [61] F. Reckermann, M. Leijnse, M. R. Wegewijs, and H. Schoeller, *Europhys. Lett.* **83**, 58001 (2008).
- [62] T. Frederiksen, K. J. Franke, A. Arnau, G. Schulze, J. I. Pascual, and N. Lorente, *Phys. Rev. B* **78**, 233401 (2008).

- [63] M. G. Schultz, T. S. Nunner, and F. von Oppen, *Phys. Rev. B* **77**, 075323 (2008).
- [64] J. Repp, P. Liljeroth, and G. Meyer, *Nat. Phys.* **6**, 975 (2010).
- [65] J. C. Cuevas and E. Scheer, *Molecular Electronics: An Introduction to Theory and Experiment* (World Scientific, Singapore, 2010).
- [66] M. Tsuchiizu, Y. Omori, Y. Suzumura, M.-L. Bonnet, and V. Robert, *J. Chem. Phys.* **136**, 044519 (2012).
- [67] R. Härtle, C. Benesch, and M. Thoss, *Phys. Rev. B* **77**, 205314 (2008).
- [68] F. A. Cotton, G. Wilkinson, C. A. Murillo, and M. Bochmann, *Advanced Inorganic Chemistry: A Comprehensive Text* (Wiley-Interscience, New York, 1999).
- [69] M. Čížek, M. Thoss, and W. Domcke, *Phys. Rev. B* **70**, 125406 (2004).
- [70] U. Peskin, *J. Phys. B* **43**, 153001 (2010).
- [71] G. D. Mahan, *Many-Particle Physics* (Plenum, New York, 1981).
- [72] M. Galperin, A. Nitzan, and M. A. Ratner, *Phys. Rev. B* **73**, 045314 (2006).
- [73] V. May, *Phys. Rev. B* **66**, 245411 (2002).
- [74] J. Lehmann, S. Kohler, V. May, and P. Hänggi, *J. Chem. Phys.* **121**, 2278 (2004).
- [75] U. Harbola, M. Esposito, and S. Mukamel, *Phys. Rev. B* **74**, 235309 (2006).
- [76] R. Volkovich, M. Caspary Toroker, and U. Peskin, *J. Chem. Phys.* **129**, 034501 (2008).
- [77] R. Härtle, R. Volkovich, M. Thoss, and U. Peskin, *J. Chem. Phys.* **133**, 081102 (2010).
- [78] S. Nakajima, *Prog. Theor. Phys.* **20**, 948 (1958).
- [79] R. Zwanzig, *J. Chem. Phys.* **33**, 1338 (1960).
- [80] R. Härtle and A. J. Millis, *Phys. Rev. B* **90**, 245426 (2014).
- [81] C. Schinabeck, R. Härtle, H. B. Weber, and M. Thoss, *Phys. Rev. B* **90**, 075409 (2014).
- [82] T. Böhler, J. Grebing, A. Mayer-Gindner, H. Löhneysen, and E. Scheer, *Nanotechnology* **15**, S465 (2004).
- [83] M. Elbing, R. Ochs, M. Koentopp, M. Fischer, C. von Hänisch, F. Weigend, F. Evers, H. Weber, and M. Mayor, *Proc. Natl. Acad. Sci. USA* **102** 8815 (2005).
- [84] N. J. Tao, *Nat. Nano* **1**, 173 (2006).
- [85] Z. K. Keane, J. W. Ciszek, J. M. Tour, and D. Natelson, *Nano Lett.* **6**, 1518 (2006).
- [86] Y. Xue and M. A. Ratner, *Phys. Rev. B* **68**, 115406 (2003).
- [87] F. Evers, F. Weigend, and M. Koentopp, *Phys. Rev. B* **69**, 235411 (2004).
- [88] C. R. Arroyo, T. Frederiksen, G. Rubio-Bollinger, M. Véllez, A. Arnau, D. Sánchez-Portal, and N. Agrait, *Phys. Rev. B* **81**, 075405 (2010).
- [89] D. A. Ryndyk, M. Hartung, and G. Cuniberti, *Phys. Rev. B* **73**, 045420 (2006).
- [90] J. Koch, M. Semmelhack, F. von Oppen, and A. Nitzan, *Phys. Rev. B* **73**, 155306 (2006).
- [91] R. Leturcq, C. Stampfer, K. Inderbitzin, L. Durrer, C. Hierold, E. Mariani, M. G. Schultz, F. von Oppen, and K. Ensslin, *Nat. Phys.* **5**, 327 (2009).
- [92] R. Härtle and M. Thoss, *Phys. Rev. B* **83**, 125419 (2011).
- [93] R. Härtle, G. Cohen, D. R. Reichman, and A. J. Millis, *Phys. Rev. B* **88**, 235426 (2013).
- [94] H. Park, J. Park, A. K. L. Lim, E. H. Anderson, A. P. Alivisatos, and P. L. McEuen, *Nature (London)* **407**, 57 (2000).
- [95] L. P. Kouwenhoven, D. G. Austing, and S. Tarucha, *Rep. Prog. Phys.* **64**, 701 (2001).
- [96] S. Sapmaz, P. Jarillo-Herrero, Y. M. Blanter, and H. S. J. van der Zant, *New J. Phys.* **7**, 243 (2005).
- [97] D.-H. Chae, J. F. Berry, S. Jung, F. A. Cotton, C. A. Murillo, and Z. Yao, *Nano Lett.* **6**, 165 (2006).
- [98] J. M. Thijssen and H. S. J. Van der Zant, *Phys. Status Solidi B* **245**, 1455 (2008).
- [99] S. Ballmann and H. B. Weber, *New J. Phys.* **14**, 123028 (2012).